

LA-UR-08-06631

Approved for public release;
distribution is unlimited.

<i>Title:</i>	Dynamic Characterization of Carbon Foils for Space Flight Applications
<i>Author(s):</i>	Anthony D. Puckett Trevor H. Collins Ryan D. Hodge John B. Lee
<i>Intended for:</i>	IMAC XXVII, A Conference and Expo on Structural Dynamics February 9-12, 2009 Orlando, FL



Los Alamos National Laboratory, an affirmative action/equal opportunity employer, is operated by the Los Alamos National Security, LLC for the National Nuclear Security Administration of the U.S. Department of Energy under contract DE-AC52-06NA25396. By acceptance of this article, the publisher recognizes that the U.S. Government retains a nonexclusive, royalty-free license to publish or reproduce the published form of this contribution, or to allow others to do so, for U.S. Government purposes. Los Alamos National Laboratory requests that the publisher identify this article as work performed under the auspices of the U.S. Department of Energy. Los Alamos National Laboratory strongly supports academic freedom and a researcher's right to publish; as an institution, however, the Laboratory does not endorse the viewpoint of a publication or guarantee its technical correctness.

Dynamic Characterization of Carbon Foils for Space Flight Applications

Trevor Collins¹, Ryan Hodge², John Lee³, Anthony Puckett⁴

¹ Dept. of Mechanical Eng., New Mexico State University, Las Cruces, NM 88003

² Dept. of Mechanical Eng., Rose-Hulman Institute of Technology, Terre Haute, IN 47803

³ Dept. of Mechanical Eng., Oklahoma Christian University, Edmond, OK 73013

⁴ W Division, Los Alamos National Laboratory, Los Alamos, NM 87545

NOMENCLATURE

a	–	width in the case of a rectangular membrane (m)
b	–	height in the case of a rectangular membrane (m)
E	–	kinetic energy
e^-	–	secondary electron
l	–	distance that wave travels (width or height in the case of a rectangular membrane) (m)
L	–	time-of-flight (TOF) distance
m	–	mass
m,n	–	mode indexes in the a and b directions, respectively (can only be integer values)
P	–	tension (N)
T	–	temperature (C)
V^-	–	lower voltage on particle analyzer
v	–	wave velocity through membrane (m/s)
v	–	velocity of a particle
V^+	–	upper voltage on particle analyzer
μ	–	areal density (kg/m^2)
ω	–	natural frequency (rad/s)

ABSTRACT

Carbon foils are often used as part of a mass spectrometer. When a particle passes through the foil a secondary electron is generated, which can be detected by a channel electron multiplier. For mass spectrometers used in space applications, the foils must survive the large acoustic loads generated from the launch vehicle. The additional protection from a door is avoided if possible because it adds mechanical complexity and weight to the space vehicle. The goal of this research project was to further the understanding of carbon foils under dynamic loads by generating a finite element model that could be used for future carbon foil design and analysis. Experiments were conducted on the foil with an acoustic loading from a speaker. A laser vibrometer measured the vibration and modal response of the foil. In addition, a finite element model was generated, and the modal response of the membrane was computed. A sensitivity analysis was performed to determine the most influential input parameters to the finite element model. The natural frequencies measured in the experiments were used to calibrate the finite element model and provided a baseline for future dynamic modeling of the carbon foils.

1 INTRODUCTION

Carbon foils are used in a variety of applications including nuclear, optical, chemical, and microscopic research. For the purpose of this paper, however, particular attention is paid to space flight applications. Many space flight instruments incorporate carbon foils because of their ability to emit a secondary electron as ions or neutral atoms pass through them. These space instruments are often time-of-flight ion mass spectrometers, energetic neutral

atom imagers, and energetic particle detectors [1]. Figure 1 shows a simple mass spectrometer with the particle path outlined by the dashed red line. The particle energy analyzer only allows particles with a predetermined energy to pass through the analyzer. A time-of-flight (TOF) measurement provides the time that a particle takes to travel a specified length (L). When the particle passes through the carbon foil a secondary electron (e^-) is split off, which starts and stops the timer at the beginning and end of the TOF respectively. Once the particle has completely traveled through the mass spectrometer, the energy and velocity of the particle have been determined. Solving the kinetic energy equation, $E = \frac{1}{2}mv^2$, for the mass of the particle allows one to identify the particle species.

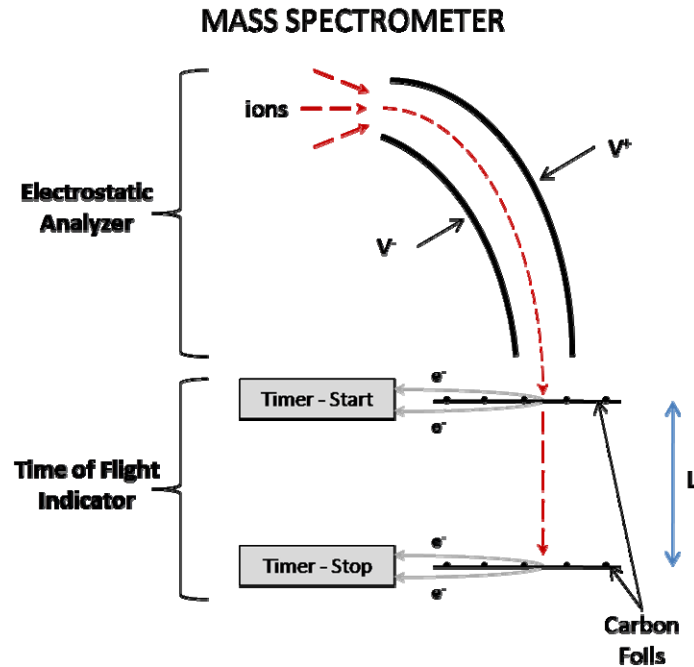


Figure 1. Mass Spectrometer

The carbon foils used in these mass spectrometers are very thin to allow particles to penetrate through the foil, but still generate a secondary electron. These thin foils are supported on a nickel grid, which is held tight by a stainless steel holder, Figure 2. The carbon foils are produced by vacuum evaporation of carbon (areal density of $0.2 \mu\text{g}/\text{cm}^2$ up to $10 \mu\text{g}/\text{cm}^2$) onto a glass substrate that has been coated with a surfactant or parting agent. The carbon foil is then floated off the substrate onto the surface of a liquid where it is picked up by a nickel grid that has been stretched on a ring. A stainless steel foil holder of the correct geometry is then placed under the nickel grid, and a stainless steel shim is welded on top clamping the nickel grid (excess material is cut away).

The nickel grids that support the carbon foils are defined by the number of lines per inch and a wide variety of sizes are used in fabricating carbon foils. The more lines per inch in a nickel grid, the less likely tears in the carbon are to occur. Tears in the carbon foil are usually the result of high stresses in the panes of the membrane. A less common but more severe tear is one that forms in the edge of the nickel grid due to fatigue and/or high stresses. These high stresses can occur during launch when vibrations in the fairings, engines, and spacecraft generate pressure waves. Vibration and acoustic levels during launch can reach 10.4 to 16.6 Grms from 20 to 2000 Hz and 140 to 146 dB from 31.5 to 10000 Hz, respectively. Figure 3 shows the sound pressure levels experienced in the Atlas V rocket at frequencies ranging from 32 to 10000 Hz.

In past launches, the most common solution to this problem was to install a retractable door or shield to protect the carbon foils during the launch sequence. The door would then be opened after the instrument was in orbit. This solution has proven quite effective [1]. Unfortunately, the addition of a protective door adds unwanted mechanical complexity to the system, which increases costs and the weight of the system. Therefore, the advancement in the understanding of how carbon foils react to various acoustic loads may eliminate the need for a protective door in some future instruments.

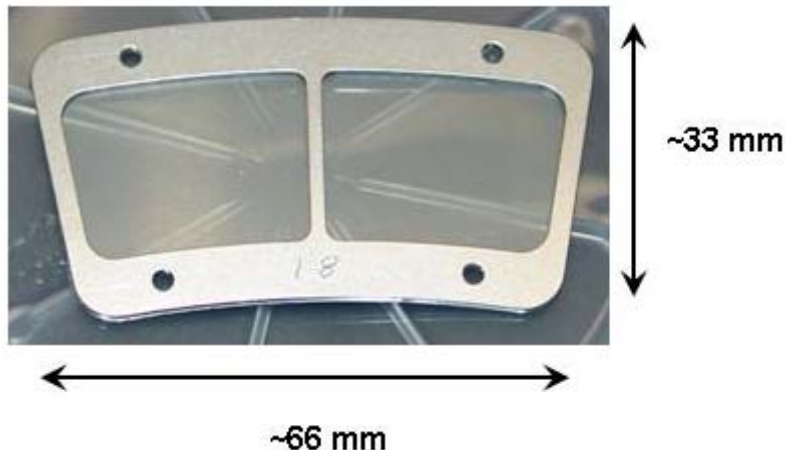


Figure 7. Example of a carbon foil assembly with nickel grid and stainless steel foil holder.

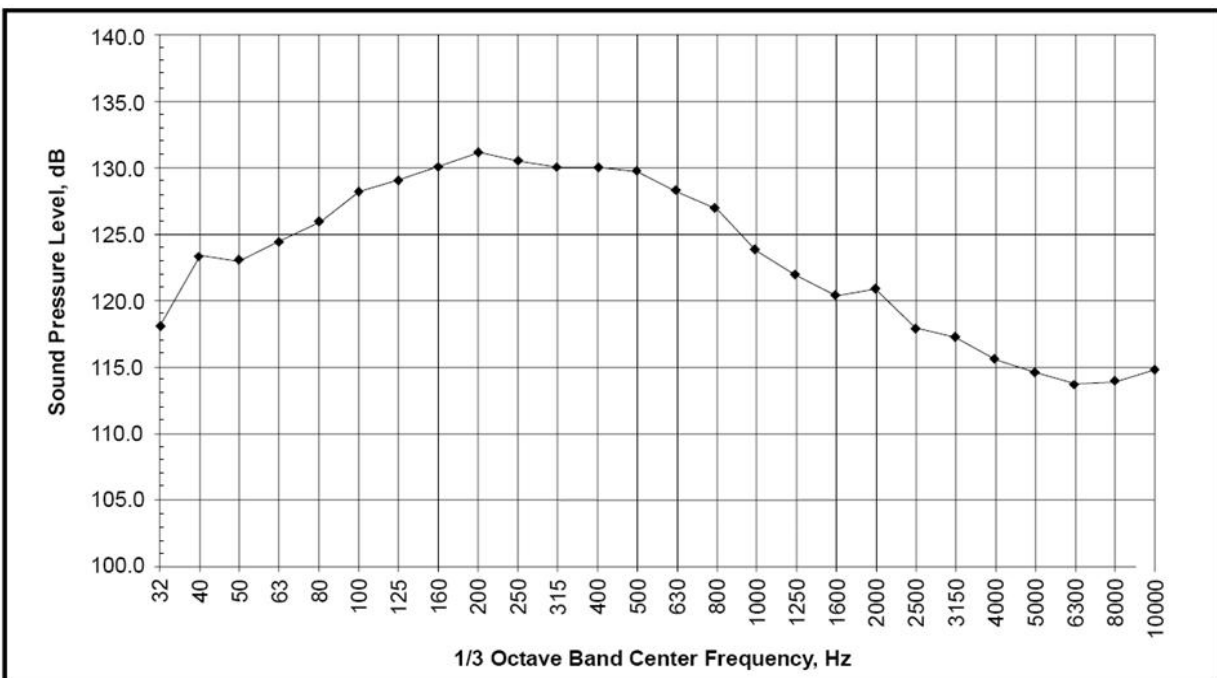


Figure 3. Atlas V Launch Environment [2]

The main objective of this research project was to advance the understanding of the dynamic response of carbon foils by generating a finite element model of the carbon foil that could be used for dynamic analysis. The modal response of the carbon foils was chosen as a means of calibrating the finite element model of the carbon foil. Experiments were conducted on the foil with an acoustic loading provided by a speaker and velocity measurements provided by a laser vibrometer. A finite element model was generated with shell elements and the modal response of the membrane was computed. A sensitivity analysis was performed to determine the most influential input parameters to the finite element model. Finally, the natural frequencies measured in the experiments were used to calibrate the finite element model and provided a baseline for future dynamic modeling of the carbon foils.

2 EXPERIMENTAL PROCEDURES

The basic experimental setup for the characterization of the carbon foils consisted of a speaker to apply an acoustic load on the carbon foil and a laser vibrometer to measure velocity. An optical table was used as a base for the experiment and allowed for positioning the foil holder in front of the speaker. Optical stages were used to scan the laser vibrometer across the carbon foil. The carbon foil and foil holder used for these experiments was very similar to the foil and foil holder in Figure 2. The foil holder was approximately 72 mm by 36 mm, and each of the two foils was approximately 22 mm by 28 mm. For these foils, $0.5 \mu\text{g}/\text{cm}^2$ areal density carbon was floated on a 333 lines/inch (13.1 lines/mm) nickel grid.

2.1 Experimental Setup Characterization

A characterization of the experimental setup was initially performed to identify anything that might influence the measurements on the carbon foil. The acoustic loading source was a 10-inch speaker enclosed in a medium-density fiberboard box and was driven by a stereo amplifier. The speaker was characterized with a microphone and a laser vibrometer to determine its own natural frequencies and how the sound pressure level changed in conjunction with these frequencies. A Dactron data acquisition unit running the RT Pro software provided a swept sine wave output to the speaker amplifier. Figure 4 shows how the system was set up for these measurements. The specific equipment used for all of these experiments is listed in Table 1.

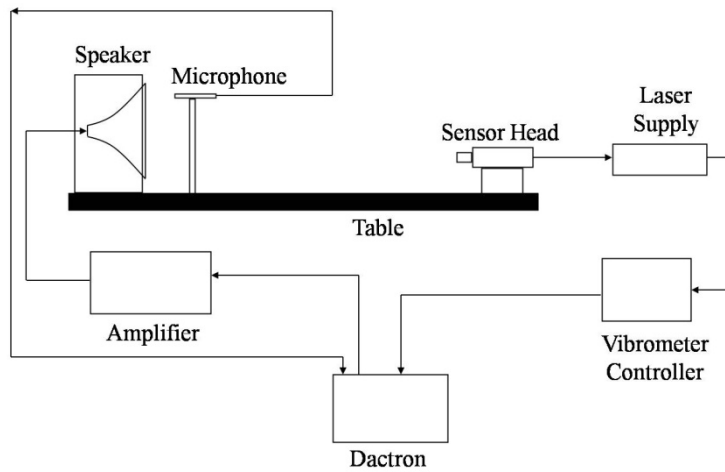


Figure 4. Configuration for Speaker Characterization Test

Table 1: Experiment equipment list

Equipment	Model #	Notes
Laser Vibrometer Controller	Polytec OFV-2500	
Laser Unit (Supply and Sensor Head)	Polytec OFV-534	
10" Hybrid Speaker	Morel H10.1 W-49-03-201	Enclosed in 10.5"x12"x12" MDF box
Data Acquisition Unit	Dactron Photon	Used with RT Pro software
Stereo Amplifier	RCA Professional Series STAV-4180 Receiver	
Shaker	Labworks Inc. ET-132	
Shaker Amplifier	Labworks PA-138-1	
Microphone	PCB 130D	

The vibration data collected by the laser vibrometer was first used to characterize the response of the speaker. Multiple measurements were made over the surface of the speaker, and an animation of the velocity data using ME'scopeVES™ indicated a uniform displacement over the area of the speaker.

The data from the microphone was used to understand the sound pressure spatially and over the frequency range of interest. For the first set of tests the microphone was placed in three different locations. For each location, the sound pressure level was recorded at six volume levels to correlate the amplifier settings to the data. As seen in 5, the sound pressure increased in a linear fashion as the amplifier setting was increased with only slight variations in the location. The recorded sound pressure did slightly increase with frequency, but each frequency was linear with amplitude.

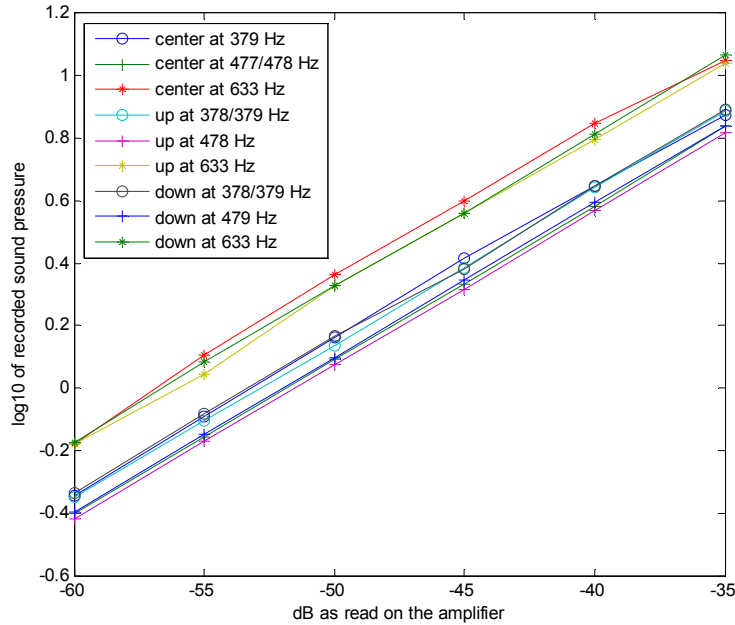


Figure 5. Recorded Sound Pressure of Speaker at Three Positions

The second part of the testing had one microphone position, 42 mm (1.65 inches) away from the center of the speaker. This test was to verify an absence of nonlinearity as frequency was swept through a broad range. The broad range was split up into five tests to produce a large set of data points and better precision. As seen from Figure 6 (left), the sound pressure was constant throughout the frequency range. The figure showed solid strips with slight indentations from aliasing. The spectrogram (right) in Figure 6 did not expose any unwanted harmonics and showed a linear acoustic output. The extra parallel lines are an artifact of the windowing used in the spectrogram.

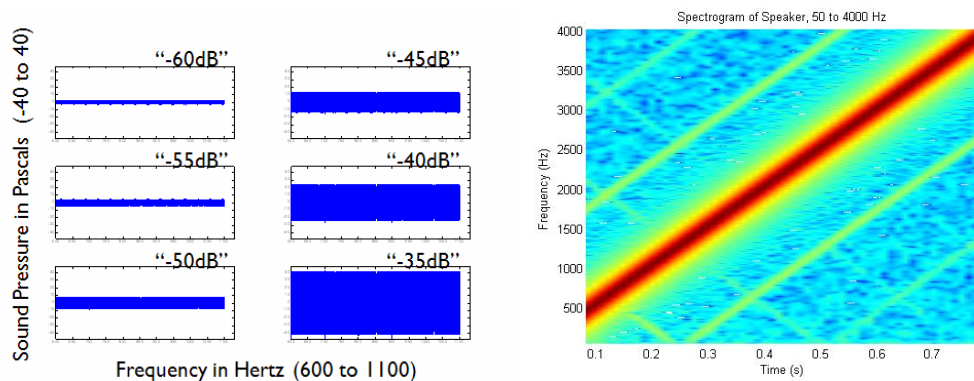


Figure 6. Sound pressure at different volume setting (left) and a spectrogram of the data

2.2 Foil Characterization

The same experimental setup was used for characterizing the foil, but with the laser vibrometer measuring the response of the foil membrane. Fortunately, the carbon foil provided sufficient reflection to the laser vibrometer, so no surface alterations were needed on the carbon foil. The modal response of the foil was needed to calibrate a finite element model, so multiple measurements were taken over the area of the foil. The left diagram in Figure 7 shows the points across the foil where velocity data was measured. Initial tests considered the foil directly in front of the speaker and a sine sweep was used for the excitation. Unfortunately, this configuration produced very poor data with the foil exhibiting the first breathing mode at all frequencies, which in hindsight is not unexpected. A number of changes were tried to improve the data, and it was found that covering a portion of the foil (but not inhibiting its movement) improved the data. Additionally, the speaker was angled relative to the foil and a burst random was used for the excitation. The right two pictures in Figure 7 show the foil assembly clamped in place with the speaker positioned to acoustically excite from an angle. Also note in Figure 7, a large section of the foil was covered so that the breathing or first bending mode would not dominate the frequency response function. Three testing configurations were considered for covering the carbon foil in the experiments, Figure 8.

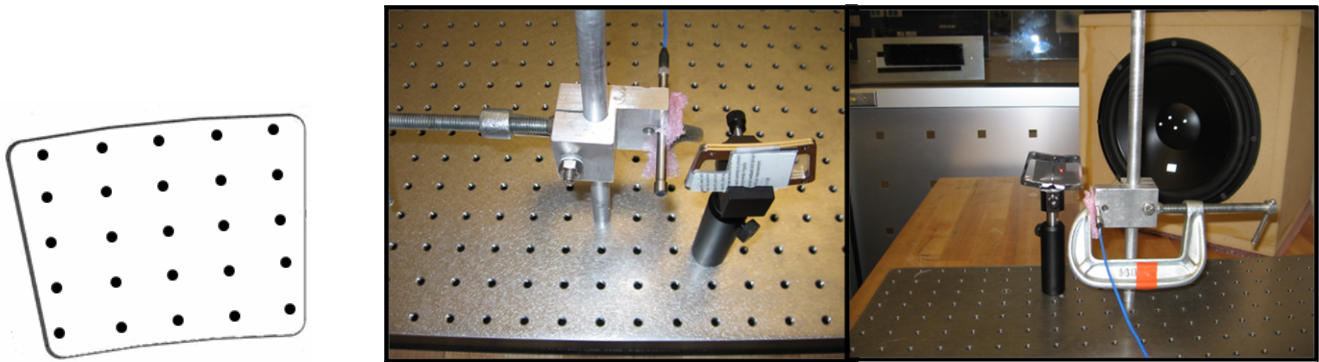


Figure 7. Velocity sampling locations (left) and the experimental setup for the foil characterization

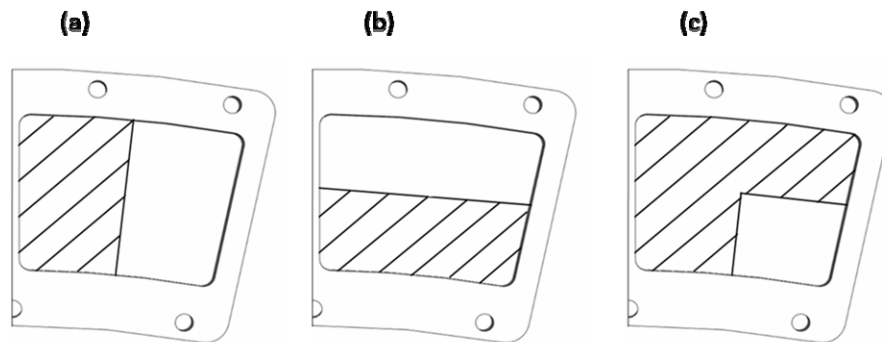


Figure 8. Three testing configurations. Hatched area marks covered sections of the Foil

3 NUMERICAL ANALYSIS

The objective of this research was to develop a finite element model capable of predicting the dynamic response of the carbon foil due to the acoustical loads. The modal response of the carbon foil was used as the means of calibrating the model. Only the foil was considered in the finite element model; the stainless steel foil holder was treated as a fixed displacement boundary condition.

3.1 Foil Finite Element Model

The nickel grid supporting the foil was 1 in² with 333 lines/in, so it was too fine to model directly without using a great deal of computing resources. Instead, an equivalent shell model was used to represent the nickel grid, Figure 9. In order for the shell model to have the same dynamic response, equivalent mass and stiffness

properties had to be calculated. The elastic modulus, thickness, and stiffness all influence the response of the foil. However, there are only two equations for the three unknowns[†]. Thus the modulus was fixed at 207 GPa, then the cross sectional area was calculated, and finally the density was calculated. The carbon layer of the foil was so thin ($0.5 \mu\text{g}/\text{cm}^2$) compared to the nickel grid ($1353 \mu\text{g}/\text{cm}^2$) that it was ignored.

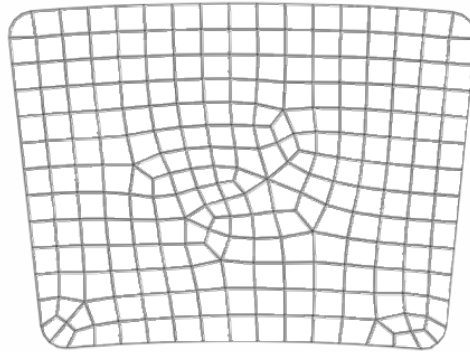


Figure 9. Foil Finite Element Mesh

The properties of the nickel grid used in the carbon foils are listed in Table 2 [3]. These properties were used to calculate the equivalent cross-sectional area and the equivalent density. Figure 10 shows the equivalent shell thickness for equal cross-sectional areas (top) and the equivalent grid area for the density calculation (bottom). Using the original density of nickel as $8880 \text{ kg}/\text{m}^3$, the density of the shell was calculated to be $16310 \text{ kg}/\text{m}^3$ by equating the volumes. These equivalent properties created a starting point for modeling the carbon foil for modal analysis purposes.

Table 2: Nickel Grid Specifications

Wires (per in)	Hole Size (μm)	Wire Width (μm)	Wire Thickness (μm)
333	64	12.4	5.08

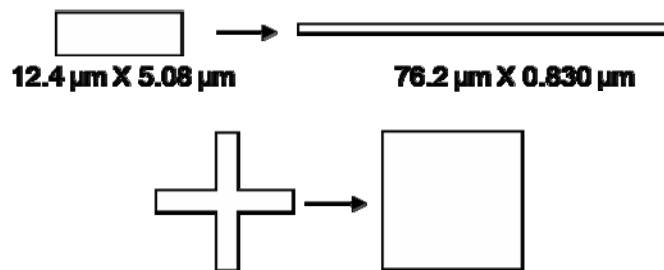


Figure 10. Equating cross-sectional area (top) and grid area (bottom) from grid to shell.

The manufacturing process of the carbon foil includes tensioning the nickel grid. In the finite element model, the tension was applied by the means of a thermal step. The edges of the foil were fixed, and the temperature was dropped to create a uniform strain and thereby tension in the foil. An arbitrary coefficient of thermal expansion, α , was chosen, $133.33 \mu\text{m}/\text{m}^\circ\text{C}$, and the temperature change, ΔT , was adjusted to apply different levels of strain/tension. Based on limited knowledge about the stretching of the nickel grid and known nickel material properties, it was estimated that a reasonable tension involved would be associated with a stretching of .02 mm

[†] The equation for the equivalent normal stress is linearly dependent to the equation for equivalent bending stress.

on a 150 mm diameter piece of grid. This equates to a strain of 0.01333% and a tension of 22.9 N/m[‡], and it provides a starting point for evaluating the shell model.

The equivalent cross sectional area and elastic modulus of the shell model ensured that the tension-strain relation in the shell model corresponded to the tension-strain relation in the nickel grid, equations 1 and 2.

$$\varepsilon = \frac{P}{AE} = \alpha\Delta T \quad \text{Equation 1}$$

$$P = A_{grid} E_{grid} \alpha\Delta T = A_{shell} E_{shell} \alpha\Delta T \quad \text{Equation 2}$$

3.2 Sensitivity Analysis

The modal response and natural frequencies of the foil are a function of the thickness, density, and tension. A quick sensitivity analysis was performed to determine the sensitivity of the finite element model to these various parameters. The factors examined were the thickness, density, and tension. The values for each parameter in the finite element shell model are shown in Table 3 along with the resulting first natural frequency from each run. Using Matlab, an N-way ANOVA was performed to calculate the F-Values of each parameter. The results of this ANOVA are shown in Figure 11. The F-values show that the tension in the foil is by far the largest factor in changing the natural frequencies.

Table 3: Parameter Values for Sensitivity Analysis

Tension (N)	Thickness (μm)	Density (kg/m ³)	ω ₁ (Hz)
0.00865	0.74676	16310	139
4.32724	0.74676	16310	3111
0.00865	0.91271	16310	126
4.32661	0.91271	16310	2814
0.00865	0.74676	17941	194
4.32724	0.74676	17941	2966
0.00865	0.91271	17941	120
4.32661	0.91271	17941	2683

This result is consistent with the analytical solution for a rectangular membrane, equations 3 and 4 [4].

$$\left(\frac{\omega_{mn}}{v}\right)^2 = \left(\frac{m\pi}{a}\right)^2 + \left(\frac{n\pi}{b}\right)^2 \quad \text{Equation 3}$$

where

$$v = \sqrt{\frac{P/l}{\mu}} \quad \text{Equation 4}$$

[‡] This value is tension per cross-sectional length, which is equivalent to stress times thickness.

The equations show the natural frequencies, ω_{mn} , are a function of the tension and density and not the thickness. For the case of the carbon foil, the tension could vary much more than the density, so the tension was the most sensitive parameter.

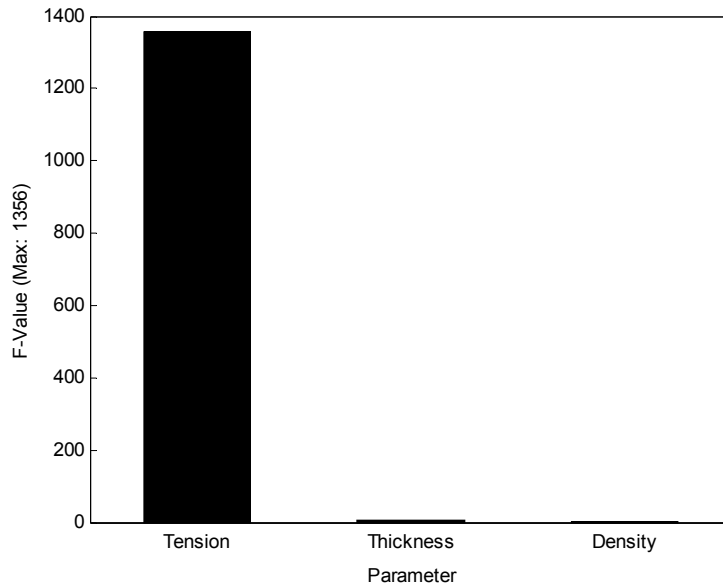


Figure 11. F-Values for Sensitivity Analysis

The finite element model was run with multiple tensions (temperature drops) to determine the relationship of the tension to the first natural frequency for the foil geometry. Using this relationship, it was then possible to calibrate the model to the experimental data by using the line equation to determine the appropriate temperature drop to match the natural frequency found by the experiment. This graph was created for each of the first three modes and the first mode is shown in Figure 12. By creating a new simulation run for each temperature drop, it allows for a range of tension values to be considered.

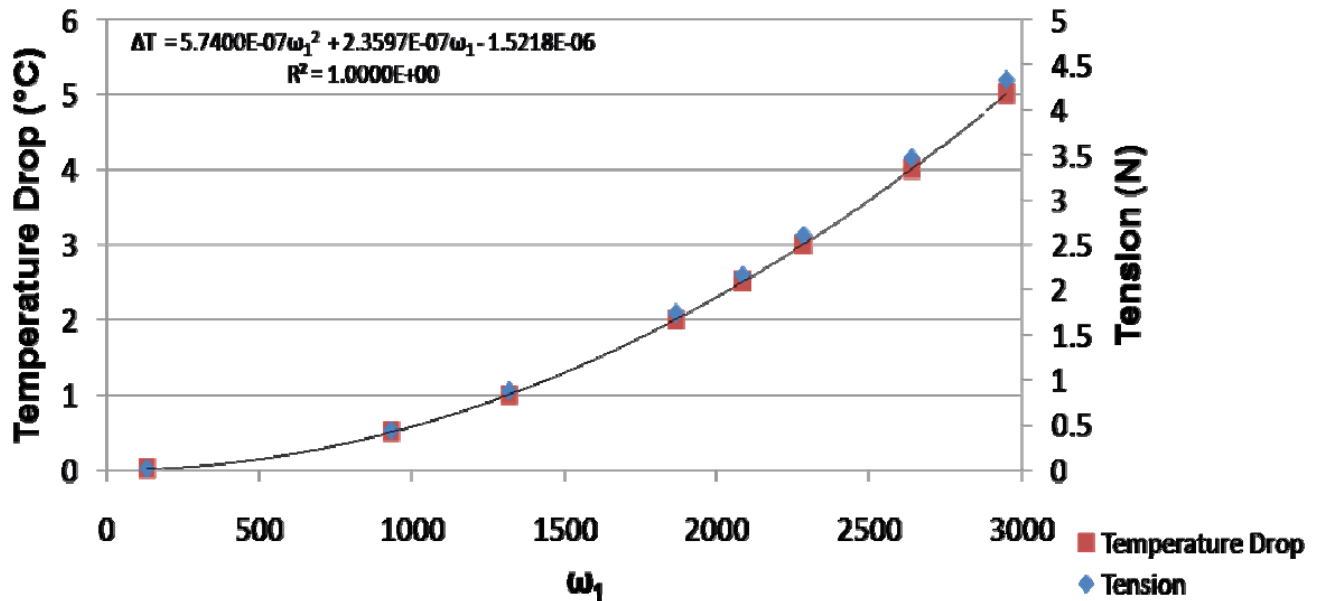


Figure 12. Correlated Temperature Drop and Vertical Tension Based on First Natural Frequency

4 RESULTS AND ANALYSIS

The tests on the carbon foil provided natural frequencies for the first three modes for the three testing configurations (Figure 8). Figure 13 shows an example of the frequency response function (FRF) and the coherence for the test where the bottom half of the foil was covered. Several peaks are apparent, but not all correspond to a vibrational mode of the foil. Fortunately, the foil geometry was close enough to a rectangle that the expected modes shapes of the foil were known. This knowledge was used to pinpoint the natural frequencies, by finding the frequency that demonstrated a vibrational mode that was the same as the anticipated mode shape. Figure 14 shows the mode shapes measured in the experiments corresponding to the first three natural frequencies. Similar data was recorded for the other testing configurations.

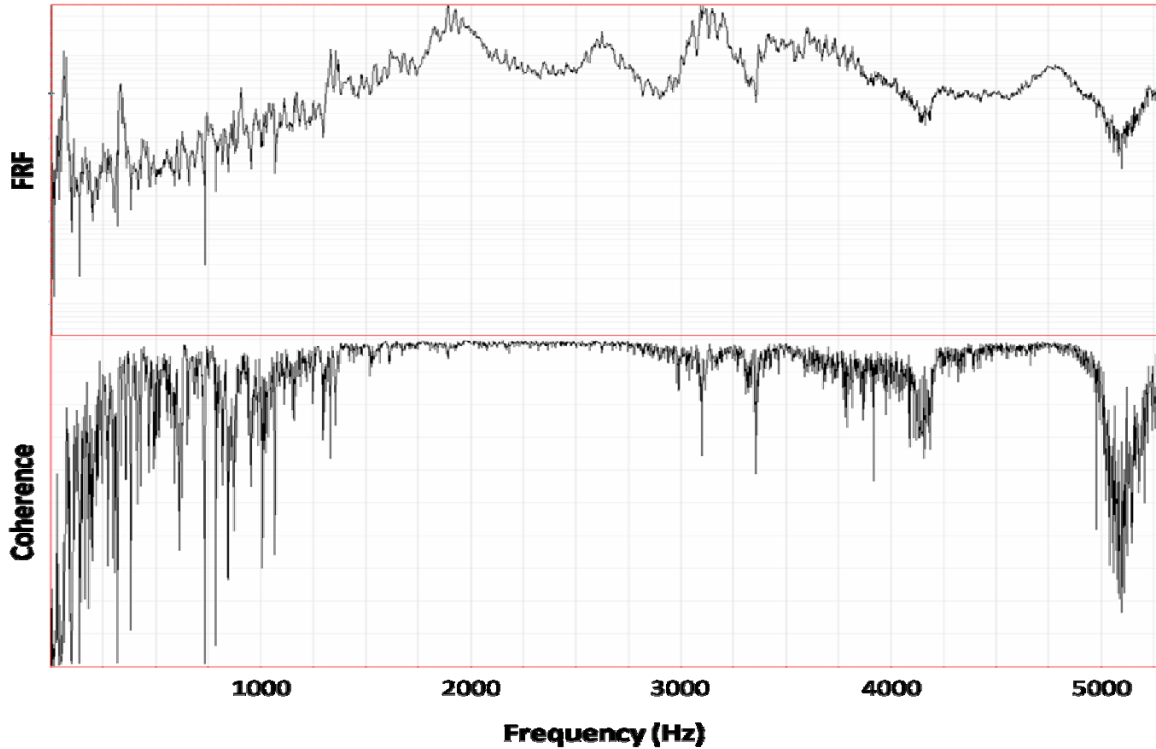


Figure 13. FRF and Corresponding Coherence of the Second Test

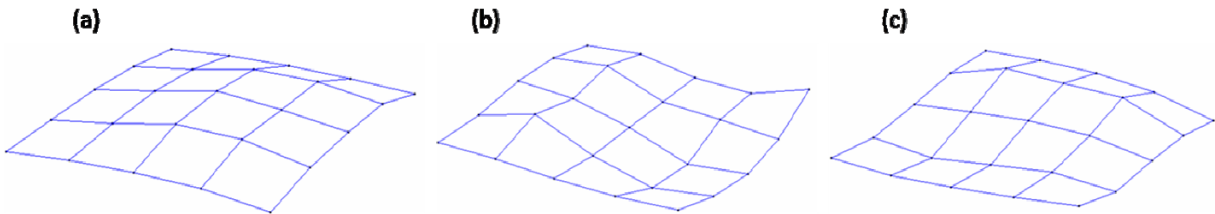


Figure 14. First three modes as seen in ME'scopeVES™

The frequencies for the first three modes are listed in Table 4 for each of the experimental tests. The natural frequencies were consistent across the experimental configurations with some variation. This fact reinforces that covering different parts of the foil did not affect the modal response, but instead subtly changed how the acoustic vibrations excited the foil. The configuration that covered the bottom half of the foil, Figure 8 (b), provided the most information, showing the clearest distinction of peaks in the frequency response function. Specifically, the second and third modes were noticeably excited. The configuration that covered the left half of the foil, Figure 8 (a), provided the worst results for the second and third modes, but had clear frequencies for the first and fourth mode. This occurrence resulted because the test configuration induced vibrations that amplified the horizontal

bending mode. The result in the frequency response function was a broader and more indistinct peak in the range of the actual second and third mode. The resulting mode shape animation appeared to be a combination of the second and third modes, bending across a diagonal. The final configuration that left only a bottom corner uncovered, Figure 8 (c), was designed to further localize the acoustic source coming in, but failed to give peaks as clear as the second configuration. Again, the frequency response function verified the same frequencies for the first and fourth modes.

Table 4: Modal Data for Three Test Configurations

	1st Mode (Breathing)	2nd Mode (Horizontal Bending)	3rd Mode (Vertical Bending)
Covering left half of foil	1940 Hertz	blending of modes at 3120 Hertz	
Covering bottom half of foil	1920 Hertz	3090 Hertz	3410 Hertz
Bottom corner of foil uncovered	1910 Hertz	3100 Hertz	3420 Hertz

The natural frequencies from the experiments were used to calibrate the finite element model. For each of the natural frequencies found in the experiments, a tension was determined from the tension-natural frequency curves previously generated. This tension was used in the finite element model. All three natural frequencies calculated in the finite element model were then compared to the experimental results. Table 5 summarizes those results.

Table 5. Results from finite element analyses when correlating the natural frequencies

	ΔT (°C)	ω_1 (Hz)	ω_2 (Hz)	ω_3 (Hz)	Tension (N/m)
Test data		1900	3120	3400	
Run 1	-2.0726	1900	2772	3220	59.3
Run 2	-2.6260	2139	3120	3624	75.2
Run 3	-2.3112	2006	2927	3400	66.2

With a limited number of results it is hard to draw many conclusions. However, these results do provide a range of tension values to consider for finite element modeling of future foils made with the same manufacturing process. Knowledge of the tension values in the foil allows one to start to consider the acoustic pressure loads and to try to determine if there will be failure in the nickel grid due to fatigue or high stress.

5 CONCLUSIONS AND FUTURE WORK

This research has advanced the understanding of the dynamic response of carbon foils and provided a technique for measuring the tension in the nickel grid supporting a carbon foil. The research demonstrated that a laser vibrometer could be used to measure the modal response of a carbon foil, and in conjunction with a finite element model, the tension in the foil could subsequently be determined. These tension values will enable future finite element analyses of different geometries to consider dynamic pressure loads.

Although, only a limited number of measurements could be taken due to time constraints (This project was part of the 9 week Los Alamos Dynamics Summer School, LADSS.), and only one carbon foil was available for testing (The foils are not cheap to make, are fragile, and no one has any spare foils.), a foundation has been laid for future work. Future work will consider multiple foils and multiple geometries to quantify the uncertainty in the tension values and to validate the finite element model of the foil.

6 ACKNOWLEDGEMENTS

We would first like to thank Los Alamos National Laboratory, in particular Chuck Farrar, for allowing us all the opportunity to work with some of the most respected names in structural dynamics. A special thanks to all the companies who donated the software packages that were utilized for this experiment. The companies and their representatives are as follows: Mark Richardson, Vibrant Technologies, Rene Sprunger, Abaqus, Inc., and Allison Groark, The Mathworks™. We would also like to thank Kevin Farinholt, for constructing the speaker box, Peter Goodwin and Israel Owens for experimental equipment and John Bernardin for providing the foil test samples.

7 REFERENCES

- [1] McComas, D. J. *et al.*, "Ultrathin (~10 nm) carbon foils in space instrumentation", Review of Scientific Information, Vol. 75 No. 11, 2004.
- [2] Gass, Michael C., "Atlas Launch System Mission Planner's Guide", Atlas V Addendum, 52, 1999
<http://spacecraft.ssl.umd.edu/design_lib/Atlas5.pl.guide.pdf>
- [3] Industrial Netting, Micro-Mesh® Electroformed Screens,
<http://www.industrialnetting.com/pdf/MICRO_MESH_DS.pdf>
- [4] Härtel, Hermann, "The vibrating-membrane problem - based on basic principles and simulations"
<<http://www.astrophysik.uni-kiel.de/~hhaertel/PUB/membrane.pdf>>